Ghoneim E, et al., J Atmos Earth Sci 1: 002
DOI: 10.24966/AES-8780/100002

HSOA Journal of Atmospheric & Earth Sciences

Research Article

Vegetation Drought Analysis in Tunisia: A Geospatial Investigation

Eman Ghoneim[1*], Alina Dorofeeva[2], Michael Benedetti[1], Douglas Gamble[1], Lynn Leonard[1] and Mostafa AbuBakr[3]

[1]Department of Earth and Ocean Sciences, University of North Carolina Wilmington, Wilmington, USA

[2]Charlotte Department of Transportation, Planning and Design Division, Charlotte, USA

[3]Geology Department, Faculty of Science, Al-Azhar University, Nasr City, Cairo, Egypt

Abstract

Drought is one of the natural hazards that has an immense impact on nations and affects many people every year. In this study, satellite remotely sensed data were employed to estimate multiple drought indices for the growing season over Tunisia for 13 successive years. The Vegetation Condition Index (NDVI), and the Land Surface Temperature (LST) index, were combined to calculate the Vegetation Health Index (VHI). Moreover, the Precipitation Condition Index (PCI) was calculated and added to form a newly modified Vegetation Temperature Precipitation Condition Index (VTPCI). The effectiveness in drought monitoring by these indices was supported by comparing them with the Food and Agriculture Organization (FAO) annual crop yield. These indices indicated that year 2002 was the driest year in Tunisia, a result that was confirmed by the crop yield statistical data. The results revealed that four governorates of the Southern Tunisia are highly prone to drought and that grassland and cropland are the most susceptible vegetation types to drought events in Tunisia. The VTPCI shows higher correlation with the annual crop yield data than the commonly used VHI index, particularly on the sub-national scale, therefore this index is recommended to be adopted to monitor vegetation drought elsewhere in semi-arid regions where surface weather data are scarce.

Keywords: Natural hazards; Satellite land surface temperature; TRMM rainfall data; Vegetation health indices

***Corresponding author:** Eman Ghoneim, Department of Earth and Ocean Sciences, University of North Carolina Wilmington, Wilmington, USA, Tel: +1 9109622795; E-mail: ghoneime@uncw.edu

Citation: Ghoneim E, Dorofeeva A, Benedetti M, Gamble D, Leonard L, et al. (2017) Vegetation Drought Analysis in Tunisia: A Geospatial Investigation. J Atmos Earth Sci 1: 002.

Received: October 12, 2017; **Accepted:** November 17, 2017; **Published:** December 04, 2017

Introduction

Although drought is a complex phenomenon, it has been defined specifically by the remote sensing community as a period of abnormally dry weather, which results in vegetation changes [1,2]. Drought is a recurring climatic process occurs with irregular temporal and spatial characteristics over an expansive region and over an extended period of time. It is among the most devastating natural disasters causing economic losses and impacting agricultural, ecological and socio-economic spheres [3,4]. Drought has become a major environmental issue in recent years, especially in semiarid regions of the northern hemisphere and is likely to intensify and become more frequent with imminent climate change [5,6]. The growing need for agricultural production and water resources has driven researchers to concentrate on drought risk assessments [7]. Therefore, several indices have been developed and widely used for monitoring the local drought conditions. The Standardized Precipitation Index (SPI) is a commonly used drought index in monitoring severe drought conditions [8]. However, SPI relies on observed precipitation data collected at meteorological stations, which are not always available in many developing regions of the world. Satellite data, on the other hand, provide temporally and spatially continuous data worldwide. As satellite-based remote sensing can consistently and continuously monitor the environment, detecting the beginning, end, and severity of droughts with satellite-derived data is becoming very popular in drought hazards, desertification and climate change studies [2,9-11,3].

Various types of satellite-based remote sensing data and remote sensing algorithms have been widely used over the past few decades to effectively monitor the drought phenomenon worldwide. For example, a remote sensing based drought study conducted on China using the HJ-1 and microwave MASR satellite data [12,10], and in India, Philippines and Australia using MODIS data [13,14], confirmed the effectiveness of such data in the national drought monitoring. Moreover, a large number of remote sensing indices based on, for instant, the NDVI-LST relationship such as Vegetation Health Index (VHI), Temperature-Vegetation Drought Index (TVDI), Vegetation Supply Water Index (VSWI), Drought Severity Index (DSI), and Normalized Vegetation Supply Water Index (NVSWI) have been proposed and successfully tested [15-18] .

Many other simple indices based on remote sensing data were proposed to monitor drought. For example, the Normalized Difference Vegetation Index (NDVI), developed by Rouse et al., [19] is based on the ratio between the maximum absorption of radiation in the red channel, due to the leaf's chlorophyll content and the maximum reflection of radiation in the Near-Infrared (NIR) channel, due to the cell structure of the leaf [20]. The Vegetation Condition Index (VCI) was introduced first by Kogan [21,22] to measure changes in NDVI signal over time. In 1995, Kogan developed TCI (Temperature Condition Index) to normalize temperature data. Later, Kogan developed another index called the Vegetation Health Index (VHI), which is a combination of VCI and TCI. Many studies were carried out in many regions worldwide to evaluate the use of VCI, TCI and VHI indices in drought monitoring [23-25].

In addition to the above remotely sensed drought indices, the inclusion of rainfall conditions is also an important factor for drought studies. The Tropical Rainfall Measuring Mission (TRMM) provides precipitation data needed for comprehensive drought analysis. Rhee et al., [26] proposed the new multi-sensor Scaled Drought Condition Index (SDCI), which combined scaled NDVI, LST and TRMM data with assigned weights (1/4 scaled NDVI + 1/4 scaled LST + 1/2 scaled TRMM). The SDCI outperformed VHI and other existing indices in the arid region of Arizona and New Mexico and also in the humid region of the Carolinas [26]. In the present study, a newly modified drought index, namely Vegetation Temperature Precipitation Condition Index (VTPCI), based on the SDCI, was developed, examined over the study area, and compared against other drought indices. The VTPCI combines the vegetation health, temperature condition and precipitation aspects in order to gain a better understanding of the drought phenomenon in the area under investigation.

The purpose of this paper is threefold. First, to evaluate the potential of a modelling based approach for the detection of vegetation areas sensitive to drought in a data-limited semi-arid nation, such as Tunisia, using information derived from satellite remote sensor data. Second, to provide information on locations at frequent threat of drought and determine which vegetation cover type is more susceptible to frequent drought risk in Tunisia. Third, to perform a comparison of the spatial occurrences of drought detected by commonly used remotely sensed indices with the newly VTPCI index and examine the efficiency of each index using annual crop yield data.

Study Area

The research was carried out in Tunisia which is located in North Africa with a total area of 164,148 km^2 and a total population of about 10.8 million (Figure 1). Agriculture plays an important role in Tunisian economy. Today, the country cultivates various types of crops such as cereals, olives, citrus fruits, sugar beets and figs. In recent years, drought has become a frequent climate disaster in the Mediterranean area, including Tunisia, and the Intergovernmental Panel on Climate Change (IPCC) expects that such drought will be more intense and frequent in this region due to climate change [27].

In recent decades, Tunisia has faced a serious water shortage caused by low annual rainfall distributed unevenly over Tunisian territory, which increases the demand for water [28]. The country can be classified into three climate zones: Mediterranean, semi-arid and arid (Köppen types Csa, Bsh, Bwh), which all experience differing water availability. In the northern Mediterranean zone, where precipitation exceeds evapotranspiration, an annual water surplus of more than 500 mm rainfall is typical [29]. In the semi-arid central part of the country, both the annual rainfall and the number of days with rain decrease progressively in a southerly direction. The semi-arid zone receives between 350 to 500 mm of rainfall annually. The southern arid zone of Tunisia experiences an annual water deficit due to low rainfall and high rates of evapotranspiration (less than 350 mm). For most of the country, weather data come from a sparse meteorological network, which has incomplete records and is not always accessible to the public. Therefore, satellite data can contribute significantly to drought monitoring in Tunisia.

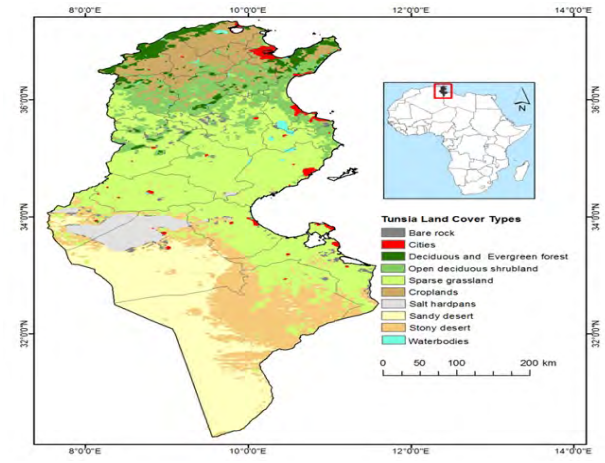

Figure 1: Location of Tunisia in North Africa and the different types of dominant land use/cover in the study area.

Data and Methods

A series of remote sensing datasets were obtained in order to calculate multiple drought indices to monitor dry conditions in Tunisia over a period of thirteen years (2000-2013). The analysis is focused on the growing season which lasts six months from November to April.

Data and pre-processing procedures

The Moderate Resolution Imaging Spectroradiometer (MODIS) Terra MOD13A3 product was used in the current study to investigate the distribution and health condition of vegetation cover for Tunisia. This product is provided monthly at a 1-km spatial resolution as a gridded level-3 product in the Sinusoidal projection. Considering the relatively large extent of the study area and a time span of 13 years, MOD13A3 spatial resolutions were considered appropriate. MODIS provides two types of vegetation indices: The NDVI and the Enhanced Vegetation Index (EVI). In this study, the EVI index was used over NDVI since it is more sensitive to changes in areas with thick vegetation cover (a shortcoming of NDVI), and capable of reducing the effect of atmospheric noise on vegetation index readings [30,31]. Previous studies indicated that the MODIS EVI index has better ability to predict crops yield than the NDVI, and the use of crop phenology information from MODIS improved the model predictability [32]. Due to this advantage, the EVI has been adopted in the present study. The EVI can be derived from the following formula:

$$EVI = G * \frac{\rho NIR - \rho \mathrm{Red}}{\rho NIR + C1 * \rho \mathrm{Red} - C2 * \rho Blue + L}$$

Where ρ are the full or partially atmospheric-corrected (for Rayleigh scattering and ozone absorption) surface reflectance; *L* is the canopy background adjustment for correcting nonlinear, differential NIR and Red radiant transfer through a canopy; *C1* and *C2* are the coefficients of the aerosol resistance term; and *L* is a gain or scaling factor. The *EVI* derived from the MODIS Terra MOD13A3 product, the following formula is used:

$$2band\ EVI = 2.5 * \frac{\rho NIR - \rho \mathrm{Red}}{\rho NIR - \rho \mathrm{Red} + 1}$$

A total of 78 EVI scenes of the study area were downloaded from the U.S. Geological Survey (http://glovis.usgs.gov/) and converted from sinusoidal projection to 1 km gridded geotiff Albers Area Projection (WGS84), using nearest neighbor resampling method. Since the objective of the study is to monitor and analyze the vegetation drought in Tunisia, a mask file of the most possible vegetation coverage was created for the study area.

For Land Surface Temperature (LST) data, the MODIS Terra MOD11A1 product, with a 1-km spatial resolution, daytime data with 8-day average coverage (four scenes per month) was used. A total of 312 MODIS-LST images were downloaded, re-projected, masked out and temperature values were converted from Kelvin to degree Celsius. Due to the cloud contamination of several LST images, the best scene out of the four available scenes for each month has been included in the analysis. Moreover, the Low-Pass filtering algorithm was applied to each scene in order to minimize the amount of missing data in some LST scenes and produce more homogeneous images [33].

Drought originates mostly from a shortage of rainfall over a protracted time period [34]. For the precipitation data, the Tropical Rainfall Measuring Mission (TRMM) 3B43 product was used to characterize rainfall amount and spatial distribution over the study area. TRMM is a joint mission between NASA and the National Space Development Agency (NASDA) of Japan and was launched on the 27th of November, 1997.

The land cover data for Tunisia were obtained from the NASA's Earth Observing System Data and Information System (EOSDIS). MODIS Land Cover MCD12Q1 product was chosen for the present study. This product provides a detailed vegetation biomass cover with a spatial resolution of 500 meters. According to the Food and Agriculture Organization (FAO) of the United Nations [35], wheat is the most extensive crop in Tunisia, which accounts for almost 80% of total production. Nation-wide annual wheat yield data were obtained from the FAO Statistical Division dataset (http://faostat3.fao.org) for the period of 2000-2013 to validate the modeled drought maps. Moreover, the annual crop yield data for the period of 2000-2008 for one of the most agro-productive regions of Tunisia, Siliana governorate, were obtained and used to estimate the efficiency of the remote sensing drought indices on the local scale [36].

Methodology

Four different types of vegetation drought indices, including the VCI, TCI, VHI and PCI, were used in this study and compared against the VTPCI modified drought index.

The VCI was first proposed by Kogan [22] and related to the long-term minimum and maximum NDVI. The assumption of VCI for drought monitoring is that a harsh drought will affect vegetation growth and result in the lowest values (closer to zero) in the multiyear observations. Conversely, the highest VCI values (closer to 100) will represent an optimal climatic condition [4]. The VCI is a pixel based normalization of the NDVI and it is calculated using the following formula (in the present study, the NDVI values were replaced with EVI ones):

$$VCI(\%) = 100 * \frac{EVI - EV\,\mathrm{Im}in}{EV\,\mathrm{Im}ax - EV\,\mathrm{Im}in}$$

EVImax and *EVImin* are the absolute multi-year maximum and minimum, respectively, calculated by the corresponding pixels in the same month from the entire EVI records (2000-2013). VCI values range between 0 and 100 (%), reflecting relative change in the vegetation condition from extreme to optimal. Monthly VCI values for the entire dataset were calculated for the study area.

The TCI, also proposed by Kogan [22], proposed that drought episode will cause a land surface thermal stress and a reduction in soil moisture which could trigger higher temperature values in the drought year than the same month of non-drought years. Accordingly, a low surface temperature in the vegetation growing season indicates more favorable conditions while high land surface temperature shows unfavorable drought conditions. The TCI can be estimated using the following formula:

$$TCI(\%) = 100 * \frac{LST\,\max - LST}{LST\,\max - LST\,\min}$$

Where *LST* is the average temperature value for the current month, *LSTmax* and *LSTmin* are the absolute maximum and minimum temperature values, respectively.

The VHI is a weighted average of the above two indices (VCI and TCI) that represents the overall vegetation health for the area under investigation [21]. The VHI can be calculated using the following formula:

$$VHI = \alpha * VCI + (1 - \alpha) * TCI$$

Where α is the coefficient quantifying the contributions of *VCI* and *TCI* in the combined condition. Since the shares of *VCI* and *TCI* are not known for any specific location, it was assumed that the shares are equal to 0.5.

While VHI has proven to be a fairly good indicator of drought conditions in low-latitudes, mainly in arid, semi-arid, and sub-humid climatic regions, this drought index only accounts for the vegetation condition and the land surface temperature [37]. As indicated earlier, abnormally low rainfall is the primary cause of drought. Therefore, the importance of the precipitation as an influencing factor should be also considered in a comprehensive drought analysis. TRMM Accumulated Rainfall in millimeters with 3-hour intervals was obtained as a set of 0.25° x 0.25° gridded data in ASCII format. These data were imported and averaged in Excel to provide a monthly rainfall data. All the monthly data were then uploaded to ArcGIS and converted to shapefiles. Using the Kriging algorithm, the point data were interpolated to provide continuous rainfall data for each month (2000-2013) in the raster format. The Kriging method estimates unknown values from observed values at surrounding locations based on regression against values of surrounding data points. This interpolation technique proved to be successful for an application with scarce precipitation data availability [38]. The Precipitation Condition Index (PCI), based on microwave remote sensed TRMM precipitation, was recently proposed by Zhang and Jia [10]. The PCI was calculated using the following formula:

$$PCI(\%) = 100 * \frac{TRMM - TRMM\,\min}{TRMM\,\max - TRMM\,\min}$$

Where TRMM, is the pixel value representing precipitation, *TRMMmin* and *TRMMmax* are the absolute minimum and maximum, respectively. During the normalization procedure, the PCI values were

linearly scaled from 0 to 100, corresponding to changes in precipitation from extremely unfavorable to optimal.

The VHI index can be used to monitor drought from vegetation and soil temperature aspects, whereas the PCI index accounts for the rainfall condition only. Until recently; however, no indices could suitably reflect the comprehensive information of drought from both meteorological and agricultural aspects. Rhee et al., [26] proposed a new remote sensing-based drought index, known as the SDCI. This index was utilized for agricultural drought monitoring in both arid and humid regions and uses multi-sensor data. SDCI performed better than existing remote sensing drought indices in the arid region of Arizona and New Mexico as well as in the humid region of the Carolinas [26]. In line with the previous SDCI, a newly modified drought index (named VTPCI) from the SDCI, was adopted in the present study. The VTPCI combines the VCI, TCI, PCI values using the following formula:

$$VTPCI = \frac{(VCI + TCI + PCI)}{3}$$

Since the relative proportions of *VCI, TCI* and *PCI* are unknown for specific locations, the *VTPCI* assumes that the shares are equal. The VTPCI derived drought maps were compared against those derived from VHIs over Tunisia.

Land Use Land Cover (LULC)

In order to estimate the impact of climate change-induced drought on different vegetation-cover types, the MODIS LULC map (MCD12Q1 product) of the region has been utilized. A total of ten classes (Figure 1), including cities, sandy desert, stony desert, water bodies, bare rocks, salt hardpans, evergreen/deciduous forest, open deciduous shrubland, sparse grassland, and croplands (with the crop cover over 50%) were extracted and incorporated in the analysis. The cropland cover was singled out and later utilized to calculate the correlation coefficients between observed crop yield and the crop areas directly affected by the extreme, severe and moderate drought conditions.

Efficiency estimation of VHI and VTPCI using crop yield data

According to Smith et al., [39], the high correlation of the NDVI taken during the growing season indicates the capability of correctly forecasting wheat yield well ahead of the end of the growing season. Whereas estimating crop yield is not the primary objective of this study, it is imperative for validating the derived remote-sensed indices including the modified drought index (VTPCI). Based on reports by UN-FAO (FAO, 2014), wheat accounts for about 80% of cereal production in Tunisia, the rest being barley and oats. The wheat is almost entirely grown under rain fed conditions. Therefore, wheat was chosen to serve as an index usefulness indicator. The country annual wheat yield data were obtained from the FAO Statistical Division dataset, whereas the annual crop yield data for the administrative district of Siliana, governorate of Tunisia, for the years 2001 through 2008, were obtained from the drought report on Tunisia by Bergaoui et al., [36]. The latter crop yield data were used for validating the derived remotely sensed drought indices at the district level.

Several researchers suggest that the variation in final crop yield is explained by plants phenological cycle [4,26,39,40]. Therefore, wheat growing stages for the Tunisia region were also considered and incorporated in the analysis. According to the USDA/Foreign Agriculture Service reports for Tunisia (www.thecropsite.com/reports/?id=3644), wheat flowering in Tunisia occurs in March, harvest follows in June/July, but most importantly, April serves as the most critical month for moisture, because plants are in their grain-fill stage and heavily rely on water to boost the grain weight. April rainfall is the most influential factor in the local farmer decision-making. Thus, yearly April drought data along with the multi-year annual mean drought data for both VHI and VTPCI were investigated in the analysis. The drought affected areas identified by VHI and VTPCI as drought-prone were calculated on a pixel basis, with the scaled index values below 30 (extreme, severe and moderate drought combined). The derived crop mask was applied to limit the analysis to agricultural areas only. Linear regression analysis was employed to investigate the strength of the correlation between the crop yield data and those areas indicated by the studied drought indices in order to estimate their effectiveness.

Results and Discussion

Spatial and temporal comparisons of remote sensing drought indices

In order to compare the spatial patterns of drought over the study region, a series of classified drought severity maps were produced for each month of the growing season for thirteen years. The widely used classification scheme of Kogan [22] was adopted in the present study. Here each index was classified into 5 categories (Table 1), which range from extreme drought (0 to 10) to no drought (≥ 40). The scaling for each index is ranged between 0 and 100, where 0 indicates the driest condition and 100 indicates the wettest. An example of the spatial distribution of the calculated indices for all March months is illustrated in figure 2. Examination of the derived VHI and PCI, smoothed with 6-month running average time series (Figure 3), revealed a similar pattern in the behavior of both indices. The examination of annual mean distribution of both indices proved that there is a moderate positive correlation between VHI and PCI indicating that higher rainfall producing healthier vegetation cover. Analysis of PCI data revealed that approximately 30% of the study area was continuously affected by extreme drought conditions for the growing seasons of 2001/2002, 2007/2008 and 2009/2010, which corresponds to the highest peaks of extreme drought marked by VHI. This observation proves the idea that drought severity relates not only to the vegetation health but also to the rainfall which plays an important role in influencing drought conditions. Therefore, it is vital to include precipitation data for the in-depth drought monitoring in order to supplement the quality of the produced results [41].

Drought Indices Values	Drought Conditions
<10	Extreme drought
10-20	Severe drought
20-30	Moderate drought
30-40	Abnormal dry
>40	No drought

Table 1: Classification of VCI, TCI, VHI, PCI and VTPCI drought indices.

A series of multi-year means were generated in order to compare spatial patterns of VHI and the newly developed VTPCI (Figure 4), which accounts for all three important aspects of drought (vegetation health, land surface temperature, and precipitation). The spatial distribution of the VTPCI over the region generally agreed with that of the derived VHI. Both indices indicated that the season 2001-02

exhibited the most extensive and extreme drought conditions over the thirteen year span. It is important to note that the extreme and severe drought area for 2001/02, derived from VTPCI, corresponds with the entire area occupied by cropland. The driest years of 2001-02 are followed by the drought-free years of 2002/03 and 2003/04. Moderate drought occurrences, highlighted by the VHI, were observed in the Mediterranean parts of the study area right above the Atlas Mountains in 2005/06. This area also overlaps with the cropland cover. The seasons of 2009/10 and 2012/13 years show drought distributed mostly in the southern and south-eastern directions. According to both VHI and VTPCI, the 2003/04, 2006/07, 2010/11 seasons were the wettest during the 13 years of observations.

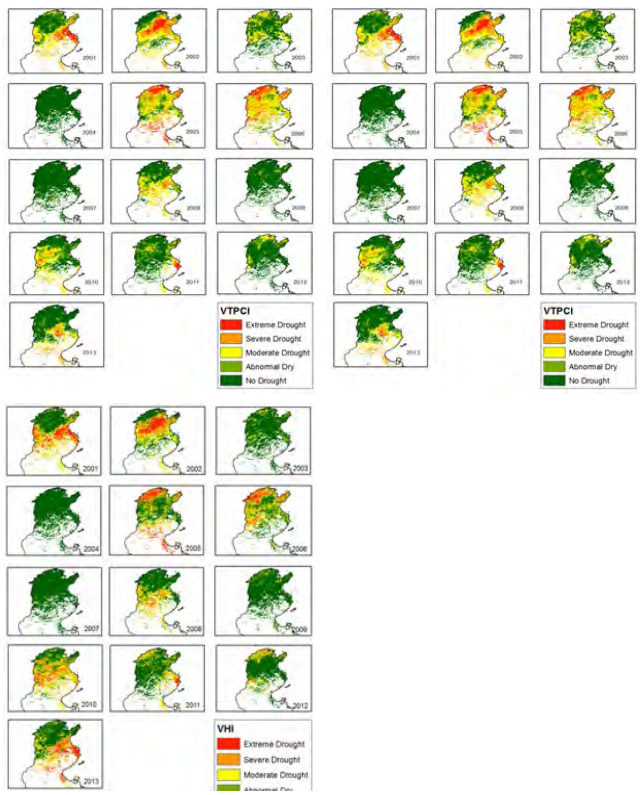

Figure 2: Distribution of VHI, PCI and VTPCI for March for years 2001 through 2013.

The year-to-year change in annual VHI and VTPCI mean values confirms these observed findings (Figure 5). The highest peaks of the annual VHI match with the highest peaks of the annual mean VTPCI values, which correspond to the wettest seasons (e.g. 2002/03, 2003/04, 2006/07, 2008/09 and 2010/11). Simultaneously, the mean VHI and VTPCI values for the 2001/02 season were the lowest throughout the whole investigation period suggesting the driest conditions throughout the study period (13 years). The drought of 2001/02 was one of the most catastrophic events for the Tunisian economy. According to the FAO report issued in 2004, the nation of Tunisia witnessed its worst drought in the past 50 years from 1999 to 2002. This catastrophe affected agricultural producers primarily. FAO statistics (http://faostat3.fao.org) verified that during the 2001/02 period the production of wheat was the lowest (14,144.05 Hg/ha), which drastically affected the local economy in Tunisia [35].

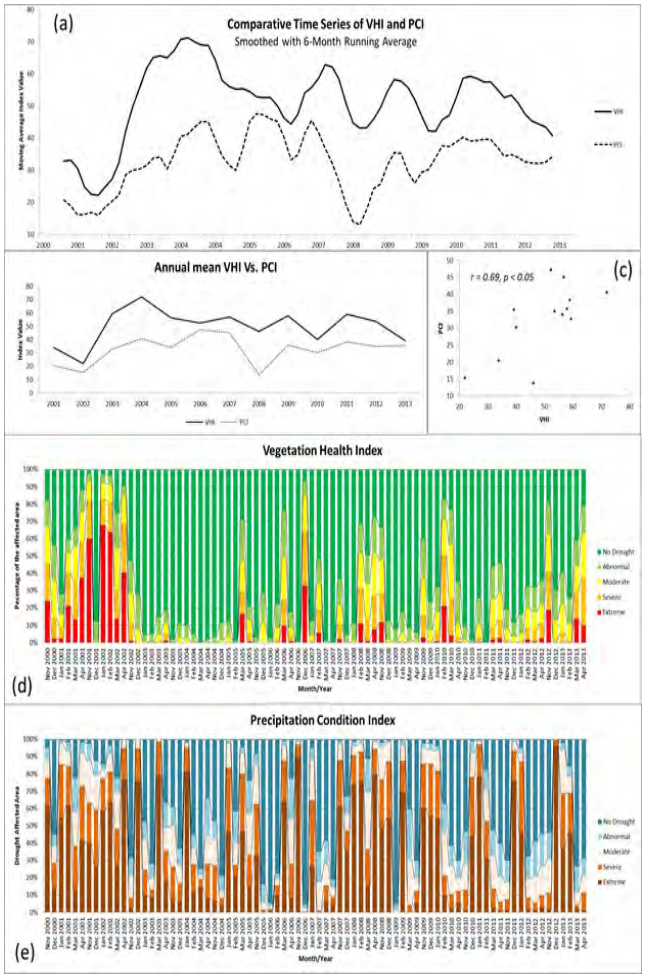

Figure 3: Temporal variations in VHI and PCI: (a) In a time series smoothed with 6-month running average (b) Annual mean VHI vs. annual mean PCI (c) The correlation scatterplot (d) Time series of proportion of study area in each drought severity category identified by VHI (e) Time series of proportion of study area in each drought severity category identified by PCI.

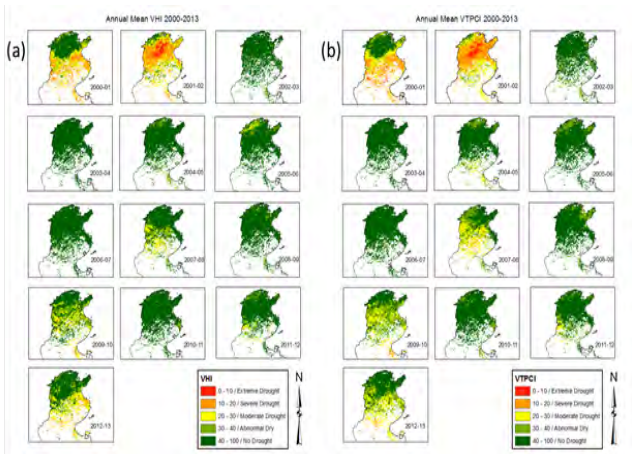

Figure 4: Spatial distribution of annual mean (a) VHI and (b) VTPCI.

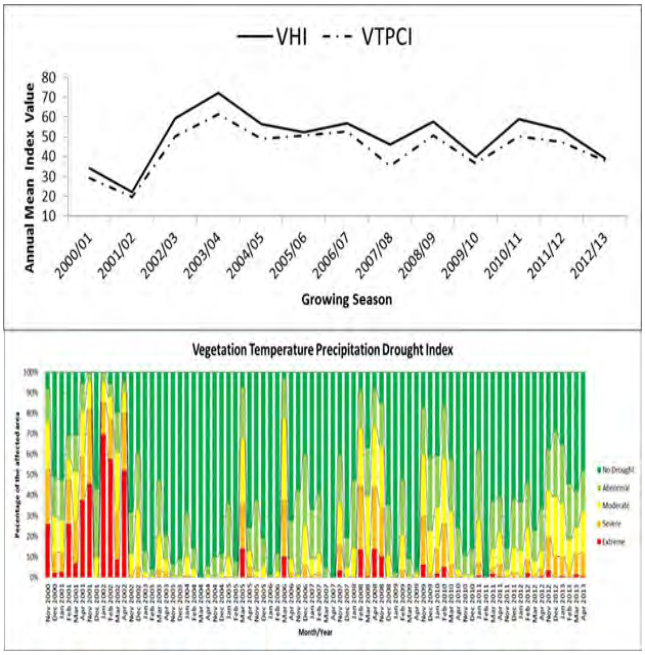

Figure 5: (a) Time series of annual mean VHI versus annual mean VTPCI, (b) Temporal distribution of mean VTPCI versus the amount of drought affected areas.

Evaluation of VHI and VTPCI using LULC and crop Yield data at the national scale

Overlaying the LULC onto VHI and VTPCI drought maps revealed that the most vulnerable vegetation type to drought conditions is sparse grassland, whereas evergreen and deciduous forest are the least susceptible to changing drought conditions (Figure 6). This can be ascribed to the fact that forest is better adapted to tolerate regular periods of water deficit and has developed structural mechanisms to cope with these conditions compared to grass (e.g., deep taproots). Neither VHI nor VTPCI indices showed peak in vegetation response for the period from 2003 to 2004, which corresponds to the wettest conditions. Despite the similarities in vegetation response, the newly modified VTPCI index, which accounts for precipitation conditions, vegetation vigor, and temperature, outperformed the commonly used VHI. VTPCI indicates better response to dry conditions for the grassland class with higher observed peaks in 2004/05, 2007/08 and 2009/10. This finding is expected since grass lifecycle is fully dependent on the amount of precipitation.

The cropland cover also appeared to be susceptible to dry conditions. Both indices generally showed similar behavior throughout the time series, with the exception of 2005/06 period, when VHI index was able to detect the cropland and the forest response to the effects of drought. Visual inspection of the annual mean VHI spatial distribution for the 2005/06 season together with the LULC, revealed that the areas affected by moderate drought lie within the cropland and the deciduous forest land cover. Both indices highlighted the 2001/02 season as the most crucial with more than 10% of the affected croplands experiencing extreme drought conditions. Both VHI and VTPCI revealed that cropland was hit hard in 2002, but it recovered quickly in 2003. This suggests that cropland is sensitive to drought, but it is also resilient and is able to recover fast.

The relevance of using VHI and VTPCI indices in terms of drought monitoring was tested through the correlation between the area affected by drought, according to VHI and VTPCI, versus the wheat yield for the entire region. Regardless of the small sample size (13 consecutive years of observations) and at a significance level (α) of 0.10, there was a moderate but significant (p = 0.08) inverse correlation, between the national crop yield and the size of the area experiencing extreme drought (Table 2). It is worth noting that many factors such as, soil quality, atmospheric conditions, water distribution, and socio-economic stability affect crop yield. Moreover, variation in crop yield is influenced by pests, diseases, fertilizers and farm management practices. Since these numerous elements affect crop yield, an absolute correlation was not expected from the computed satellite-derived indices.

Targeted Land Cover Type	Temporal Extent	Drought Index/ Severity Type	VHI	VTPCI
National Cropland Cover	Annual	0 - 30 Combined	- 0.60	- 0.56
	March	0 - 30 Combined	- 0.83	- 0.75
	April	0 - 30 Combined	- 0.34	-0.44
Sub-National Cropland Cover	Annual	0 - 30 Combined	- 0.60	- 0.56
	April	0 - 30 Combined	- 0.83	-0.85

Table 2: Linear correlation coefficients between the amount of land affected by drought versus the annual wheat yield for the entire study region. *Based on 13 observations.

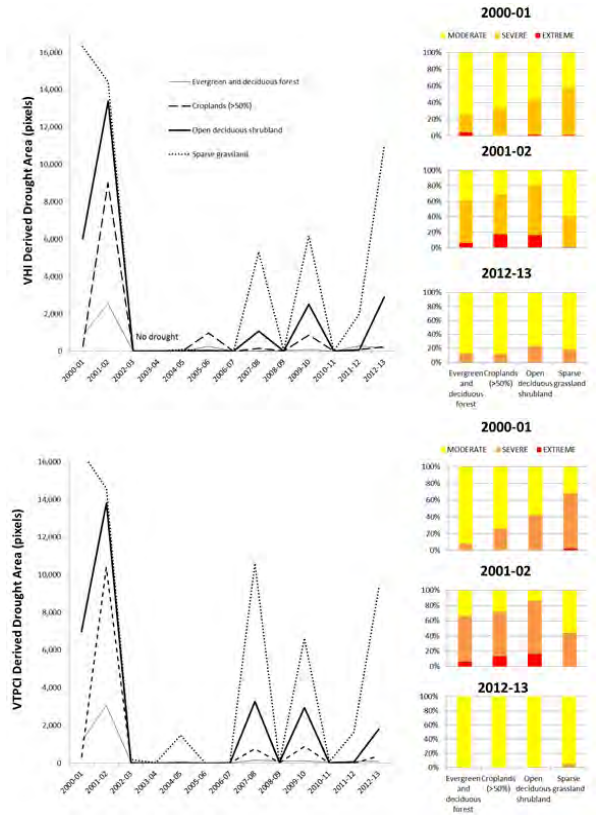

Figure 6: Vegetation response to drought derived from VHI (upper figure) and VTPCI (Lower figure). It shows that the most vulnerable vegetation type to drought conditions is sparse grassland, whereas evergreen and deciduous forests are the least susceptible to changing drought conditions.

A time series clearly shows the relationship between drought index values and crop yields over the past 13 years (Figure 7). The results show that correlation coefficient values are higher in March (-0.83 and -0.75) than April (-0.34 and -0.44) for VHI and VTPCI. This could be ascribed to wheat flowing in March. Results also indicated that VTPCI are higher in April compared to VHI which could be due to the grain filling stage when precipitation is critical. In contrast, the VTPCI is slightly lower than VHI in March, as a consequence of the excessive rainfall during the flowering stage that makes wheat more susceptible to scabs disease, as explained by Herbek and Lee [42], leading to decreased yield. Consequently, including the precipitation in the index efficiency analysis may have lowered the March correlation coefficients values.

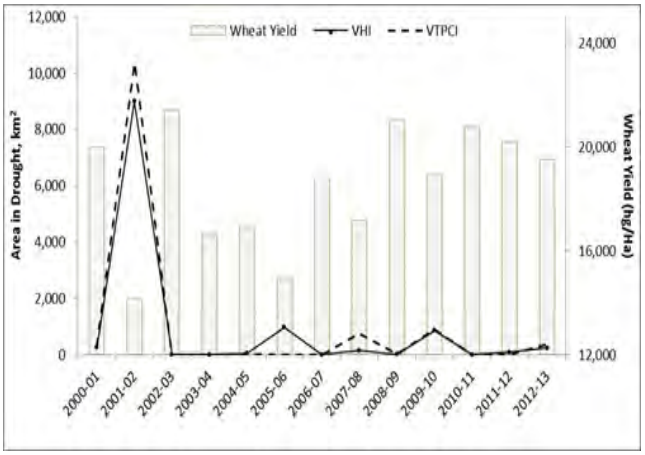

Figure 7: National wheat yield and annually averaged VHI and VTPCI for Tunisia (correlation coefficients r = -0.60 and r = - 0.56, respectively).

Comparison of VHI and VTPCI performance at the sub-national scale

As one of the most agro-productive regions of Tunisia with an annual precipitation that exceeds 400 mm [36], the Siliana governorate was chosen as the sub-national level study site. This governorate fully lies within the Medium Production Potential zone according to the FAO agricultural classification scheme. River valleys and associated floodplains make up a fifth of this governorate where floodplain soils may be moderately or severely flooded in winter. Valleys in northern sites are flood free with high agricultural potential, whereas southern locations are lightly flooded and less suitable for cultivation. As is the case at the national scale, both indices successfully identified 2001/02 as the driest season of the decade. VTPCI at the district level seems to show smoother, more continuous temporal distribution of dry conditions compared to the VHI with multiple independent drought peaks (e.g. December 2006, November 2009 etc.).

Correlation analysis showed that both VHI and VTPCI indices performed slightly better in estimating drought at the regional scale (0.61 and 0.66, respectively) than at the national scale (0.60 and 0.56, respectively). This result demonstrates the high relevance of VHI and VTPCI indexing for spatial monitoring of agricultural drought. Additionally, the VTPCI outperformed VHI in terms of correlation coefficients at both national and regional scale (Table 2). The higher correlation of April month of VTPCI (0.85) than VHI (0.83) suggests a strong negative relationship of VTPCI drought index with crop yield during the wheat grain filling stage.

Identification of drought-prone administrative districts in Tunisia

In order to identify which administrative regions of Tunisia are the most vulnerable to drought conditions, the spatial distribution of the drought indices was investigated at the regional scale, and the frequency of occurrence was compared between regions. As shown in figure 8, 3 districts of Tunisia (Tataourine, Gabes, and Gafsa) were identified as highly prone to drought and exhibited the highest level of intensity compared to other regions. These regions are located in the arid southern climate zone of the country. The northern mountainous region with prevalent Mediterranean climate was identified as less prone to suffering from extreme and severe drought conditions.

In general, these results reflect the regional climate pattern. The frequency distribution based on VHI corresponds with the major Tunisian climatic zones and the distribution of annual precipitation. Also, zones identified as highly prone to drought match the zones categorized by the FAO as having no to low production potential. Likewise, zones of the lowest probability of drought coincide with the zones classified as having medium production potential (Figure 8). Therefore, in order to perform more accurate estimation of usefulness of established drought indices the scale of the investigation was narrowed down from the entire country scale to the local sub-governorate level. Drought distribution map, shown in figure 8, reveals the higher level of detail and serves to identify drought-prone zones within the same administrative unit. For instance, Rouhia, Kesra, and El Krib were identified as the most drought-prone districts of Siliana governorate.

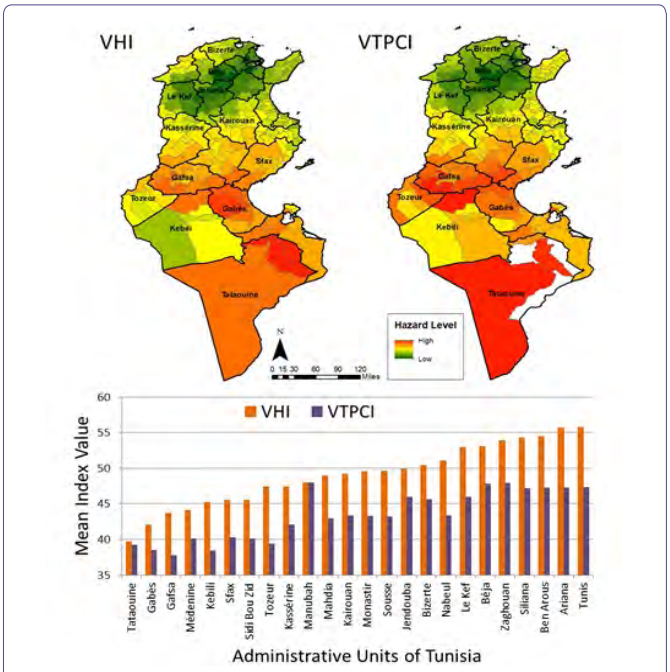

Figure 8: Distribution of VHI and VTPCI mean values within governorates and sub-governorates units of Tunisia.

Conclusion

Seasonal drought patterns in Tunisia were mapped using 400 MODIS NDVI and LST images in addition to TRMM rainfall data for the period 2000 to 2013. A total of 4 drought indices (VCI, TCI, VHI and PCI) were calculated to show the spatial and temporal distribution of extreme and severe drought in the region. A new modified drought index (VTPCI), which incorporated precipitation data along with the vegetation and surface temperature data, was developed in the present study. Results show a good correspondence between the modeled remote sensing drought data and the observed crop yield, validating the geospatial approach adopted in the present study. The newly modified index showed enhanced performance over the other indices in the study region, and outperformed the commonly used VHI on both the regional/sub-national scale. Furthermore, VTPCI is considered more effective at identifying drought over the sparse grassland and open cropland. However, the phenological cycle of wheat may have influenced the results and should be investigated further.

Remote sensing is a useful tool for drought study, particularly in large areas with limited access due to security restrictions as in the present study site (since the start of the Arab Spring in 2011). The method conducted is a low cost approach, a repeatable procedure and a viable alternative to field measurements for drought analysis and monitoring on the national scale. Tunisia witnessed its worst drought in the year 2002. This finding is consistent with the report of FAO [35], which based on analyzed tree-ring records, considered the 2002 drought to be the worst drought year in Tunisia since the mid-15th century. With this information, Tunisian officials could make informed land management decisions including where to continue with agricultural endeavors and where to protect pasture lands and forested areas. The approach used in this study allows for rapid identification of drought hotspot in Tunisia and highlights those areas and districts that are prone to extreme and severe drought. This information is essential for future agricultural and rangeland planning purposes and could be used to help decision makers enact appropriate protection measures to alleviate future drought events. The proposed procedures could be adapted, with appropriate modifications, to other countries in the Middle Eastern region.

Acknowledgment

This research did not receive any specific grant from funding agencies in the public, commercial, or not-for-profit sectors. We thank the anonymous reviewers for their thoughtful comments on this manuscript.

References

1. Heim RR (2002) A review of twentieth-century drought indices used in the United States. American Meteorological Society 83: 1149-1165.
2. Bayarjargal Y, Karnieli A, Bayasgalan M, Khudulmur S, Gandush C, et al. (2006) A comparative study of NOAA-AVHRR derived drought indices using change vector analysis. Remote sensing of Environment 105: 9-22.
3. Li X, Zhang Q, Ye X (2013) Dry/Wet Conditions Monitoring Based on TRMM Rainfall Data and Its Reliability Validation over Poyang Lake Basin, China. Water 5: 1848-1864.
4. Du L, Tian Q, Yu T, Meng Q, Jancso T, et al. (2013) A comprehensive drought monitoring method integrating MODIS and TRMM data. International Journal of Applied Earth Observation and Geoinformation 23: 245- 253.
5. Wetherald RT, Manabe S (2002) Simulation of Hydrologic changes associated with global warming. Journal of Geophysical Research 107: 1-15.
6. Trenberth K, Overpeck J, Solomon S (2004) Exploring drought and its implications for the future. EOS 85: 27.
7. Lin ML, Chen CW (2011). Using GIS-based spatial geocomputation from remotely sensed data for drought risk-sensitive assessment. International Journal of Innovative Computing, Information and Control 7: 657-668.
8. McKee TB, Doesken NJ, Kleist J (1993) The Relationship of Drought Frequency and Duration to Time Scales. Eighth Conference on Applied Climatology, Anaheim, California. 17-22.
9. Ghoneim E (2009) A Remote Sensing Study of Some Impacts of Global Warming on the Arab Region. In: Tolba MK, Saab NW (eds.). Arab Environment: Climate Change, The Arab Forum for Environment and Development (AFED), Chapter 3: 31-46.
10. Zhang A, Jia G (2013) Monitoring meteorological drought in semiarid regions using multi-sensor microwave remote sensing data. Remote Sensing of Environment 134: 12-23.
11. Ghoneim E, Mashaly J, Gamble D, Halls J, AbuBakr M (2015) Nile Delta exhibited a spatial reversal in the rates of shoreline retreat on the Rosetta promontory comparing pre- and post-beach protection Geomorphology 228: 1-14.
12. Yang B, Wang Q, Wang C, Wan H, Yang Y, et al. (2010) Drought monitoring in North China using HJ-1 satellite remote sensing data. Proceedings of the SPIE 7841.
13. Parida BR, Oinam B (2008) Drought monitoring in India and the Philippines with satellite remote sensing measurements. EARSeL eProceedings 7: 81-91.
14. Caccamo G, Chisholm LA, Bradstock RA, Puotinen ML (2011) Assessing the sensitivity of MODIS to monitor drought in high biomass ecosystems. Remote sensing of Environment 115: 2626-2639.
15. Sandholt I, Rasmussen K, Andersen J (2002) A simple interpretation of the surface temperature/vegetation index space for assessment of surface moisture status. Remote Sensing of the Environment 79: 213-224.
16. Carlson TN, Gillies RR, Perry EM (1994) A method to make use of thermal infrared temperature and NDVI measurements to infer surface soil water content and fractional vegetation cover. Remote Sensing Review 9: 161-173.
17. Mu Q, Zhao M, Kimball JS, McDowell NG, Running SW (2013) A remotely sensed global terrestrial drought severity index. Bulletin of the American Meteorological Society 94: 83-98.
18. Abbas S, Nichol N, Qamer F, Xu J (2014) Characterization of Drought Development through Remote Sensing: A Case Study in Central Yunnan, China. Remote Sensing 6: 4998-5018.
19. Rouse JW, Haas RH, Schell JA, Deering DW (1974) Monitoring vegetation systems in the Great Plains with ERTS. Proceedings, Third Earth Resources Technology Satellite-1 Symposium, Greenbelt: NASA, 309- 317.
20. Campbell JB (2006) Introduction into Remote Sensing, (4thedn). Guilford Publications, New York, USA.
21. Kogan FN (1997) Global drought watch from space. Bulletin of the American Meteorological Society 78: 621-636.
22. Kogan FN (1995) Application of vegetation index and brightness temperature for drought detection. Advances in Space Research 11: 91-100.
23. Tsiros E, Domenikiotis C, Spiliotopoulos M, Dalezios NR (2004) Use of NOAA/A VHRR-based Vegetation Condition Index (VCI) and Temperature Condition Index (TCI) for drought monitoring in Thessaly, Greece.

24. Bhuiyan C, Singh RP, Kogan FN (2006) Monitoring drought dynamics in the Aravalli region (India) using different indices based on ground and remote sensing data. International Journal of Applied Earth Observation and Geoinformation 8: 289- 302.

25. Zarei R, Sarajian M, Bazgeer S (2013) Monitoring Meteorological Drought in Iran Using Remote Sensing and Drought Indices. Desert 18: 89-97.

26. Rhee J, Im J, Carbone GJ (2010) Monitoring agricultural drought for arid and humid regions using multi-sensor remote sensor data. Remote Sensing of Environment 114: 2875 - 2887.

27. IPCC (2007) The Physical Science Basis. In: Solomon S, Qin D, Manning M, Chen Z, Marquis M, et al., (eds.). Contribution of working group I to the fourth assessment report of the Intergovernmental Panel on Climate Change. Cambridge United Press, Cambridge, United Kingdom and New York, USA. Pg no: 996.

28. Beaumont P (2002) Water policies for the Middle East in the 21st century: The New Economic Realities. International Journal of Water Resources Development 18: 315 - 334.

29. Baban Serwan MJ, Foster Ian DL, Tarmiz B (1999) Environmental protection and sustainable development in Tunisia: an overview. Sustainable Development 7: 191-203.

30. Liu HQ, Huete AR (1995). A feedback based modification of the NDV I to minimize canopy background and atmospheric noise. IEEE Transactions on Geoscience and Remote Sensing 33: 457-465.

31. Huete A, Justice C, Leeuwen WV (1999) Modis Vegetation Index (mod13) Algorithm theoretical Basis Document. The Allen Institute for Artificial Intelligence, Washington, United States.

32. Bolton KD, Friedl MA (2013) Forecasting crop yield using remotely sensed vegetation indices and crop phenology metrics. Agricultural and Forest Meteorology 173: 74-84.

33. Williamson SN, Hik DS, Gamon JA, Kavanaugh JL, Flowers GE (2014) Estimating temperature fields from MODIS Land Surface Temperature and air temperature observations in a sub-arctic alpine environment. Remote Sens 6: 946-963.

34. Knutson C, Hayes M, Phillips T (1998) How to Reduce Drought Risk. Western Drought Coordination Council, Nebraska, USA.

35. Food and Agriculture Organization of the United Nations (2004) Progress Achieved in Developing Strategies for Drought Mitigation and Preparedness Planning in the Near East Region. Food and Agriculture Organization of the United Nations, Doha, Qatar.

36. Bergaoui M, Lopez-Francos A (2010) The drought impact on agricultural crop production in Tunisia. Economics of drought and drought preparedness in a climate change context, Zaragoza, Options Méditerranéennes 95: 71-74.

37. Karnieli A, Bayasgalan M, Bayarjargal Y, Agam N, Khudulmur S, et al. (2007) Comments on the use of the Vegetation Health Index over Mongolia. International Journal of Remote Sensing 27: 2017-2024.

38. Wagner P, Fiener P, Wilken F, Kumar S, Schneider K (2012) Comparison and evaluation of spatial interpolation schemes for daily rainfall in data scarce regions. Journal of Hydrology 464-465: 388- 400.

39. Smith RCG, Adams J, Stephens DJ, Hick PT (1995) Forecasting Wheat Yield in a Mediterranean- type Environment from the NOAA Satellite. Australian Journal of Agricultural Research 46: 113-125.

40. Vicente-Serrano SM, Gouveia C, Camarero JJ, Beguería S, Trigo R, et al. (2013) Response of vegetation to drought time-scales across global land biomes. Proceedings of the National Academy of Sciences of the United States of America 110: 52-57.

41. Wan Z, Wang P, Li X (2004) Using MODIS Land Surface Temperature and Normalized Difference Vegetation Index products for monitoring drought in the southern Great Plains, USA. Remote Sensing, 25: 61-72.

42. Herbek J, Lee C (2009) A Comprehensive Guide to Wheat Management in Kentucky. Growth and Development 6-12.